WDF MODELING OF A KORG MS-50 BASED NON-LINEAR DIODE BRIDGE VCF

Maximilian Rest

E-RM Erfindungsbüro
Berlin, Germany
m.rest@e-rm.de

Julian D. Parker

Native Instruments GmbH
Berlin, Germany
julian.parker@
native-instruments.de

Kurt James Werner

The Sonic Arts Research Centre (SARC)
School of Arts, English and Languages
Queen's University Belfast, UK
k.werner@qub.ac.uk

ABSTRACT

The voltage-controlled low-pass filter of the Korg MS-50 synthesizer is built around a non-linear diode bridge as the cutoff frequency control element, which greatly contributes to the sound of this vintage synthesizer. In this paper, we introduce the overall filter circuitry and give an in-depth analysis of this diode bridge. It is further shown how to turn the small signal equivalence circuit of the bridge into the necessary two-resistor configuration to uncover the underlying Sallen-Key structure.

In a second step, recent advances in the field of WDFs are used to turn a simplified version of the circuit into a virtual-analog model. This model is then examined both in the small-signal linear domain as well as in the non-linear region with inputs of different amplitudes and frequencies to characterize the behavior of such diode bridges as cutoff frequency control elements.

1. INTRODUCTION

Modeling of electrical circuits used in music and audio devices is a topic of ongoing research in the audio signal processing domain. One particular method for modeling such circuits is the Wave Digital Filter (WDF) approach [1]. Recent work sought to expand the class of circuits that can be modeled using WDFs, focusing mainly on topological aspects of circuits [2, 3], iterative and approximative techniques for non-linearities [4, 5], methods for op-amp-based circuits [6, 7] and diode clippers [8, 9].

These developments enabled modeling a large number of circuits that were previously intractable, including guitar tone stacks [2], transistor-based guitar distortion stages [3], transistor [2] and triode [10] amplifiers, the full Fender Bassman preamp stage [11], and the bass drum from the Roland TR-808 [12].

In this paper, we examine the low-pass filter of the MS-50 synthesizer manufactured by Korg. This synthesizer was released in 1978 and intended as a companion for the more famous MS-20 model. The MS-50's filter is known primarily for exhibiting strongly nonlinear behaviors. These behaviors are due to the usage of a diode ring (similar to that seen in ring-modulators) as the cutoff controlling element in the circuit, which generates a more and more complex spectrum with rising input signal level.

Diode rings in the modulator context have been previously examined as a simplified digital model with static non-linearities [13] and as a WDF [14]. Such configurations within a filter structure have not been studied, and it is that which motivates this work.

The following paper is structured as follows: Section 2 describes the Korg MS-50 voltage-controlled low-pass filter (VCF) circuit [15] and it's core element, the diode bridge (Sec. 2.1) which is used to control the cutoff frequency. Based on a small signal linearization of this diode bridge, the Sallen-Key structure [16] of the circuit is pointed out (Sec. 2.2). In Section 3, the original circuit is reduced to the diode bridge and surrounding filter components and turned into a WDF structure. Section 4 assesses transfer functions and nonlinear behaviors of a WDF implementation in the RT-WDF framework [17] and compares them with a SPICE [18] simulation. It also evaluates the performance of the iterative Newton-Raphson Solver [4] and gives an estimate on the expected real-time requirements. Section 5 concludes the work presented here.

2. KORG MS-50 FILTER CIRCUIT

As mentioned above, in contrast to the MS-20, whose VCF is analyzed in great detail in [19], the MS-50 features a rather non-standard VCF low-pass circuit based on a biased diode bridge as the voltage controllable element to vary the cutoff frequency. This configuration has been used in Korg's 700, 700S, 800DV and 900PS synthesizers before and was covered by patent US 4039980 [20]. A contemporary reinterpretation can be found in the AM-Synths Eurorack module AM8319 Diode Ring VCF [21].

Figure 1 shows the original schematic of the filter [15]. The diode bridge is based on the RCA CA 3019 diode array [22], which features a total of six matched silicon diodes. Left of the diode bridge is the biasing circuitry and input stage. Starting from the very left of the figure, voltages from external cutoff control, manual cutoff control and a temperature compensation are added and conditioned by IC_7 into a symmetric positive and negative biasing voltage, which is fed into the two adjacent ends of the bridge. The input signal is buffered by a unity gain amplifier made of IC_6 and capacitively coupled into the input node of the bridge. Right of the bridge is the actual low-pass filter circuitry. The output signal of the diode bridge is fed into a Sallen-Key filter structure [16] with controllable resonance, high gain and amplitude limiting clipping diodes D_5–D_{12} built around IC_4. The output of this op-amp is then fed back into two additional taps in the diode bridge, which forms the necessary feedback path. This structure will be analyzed in greater detail in Section 2.2. In the rightmost part of the schematic, the signal is then differentially taken from two points in the output circuitry of the filter and passed through a DC blocking stage to the signal output. The nested configuration of diode bridge non-linearities in the feedback path of the op-amp IC_4 makes the MS-50 filter well suited for a topologically preserving modeling approach with WDFs.

2.1. Diode Bridge

The diode bridge around IC_5 in the filter structure acts as a controllable impedance element for both the input signal and the feedback path. This technique is already pointed out in the component's application note [23], and is consistent with the use of such circuits as a signal multiplier in radio applications.

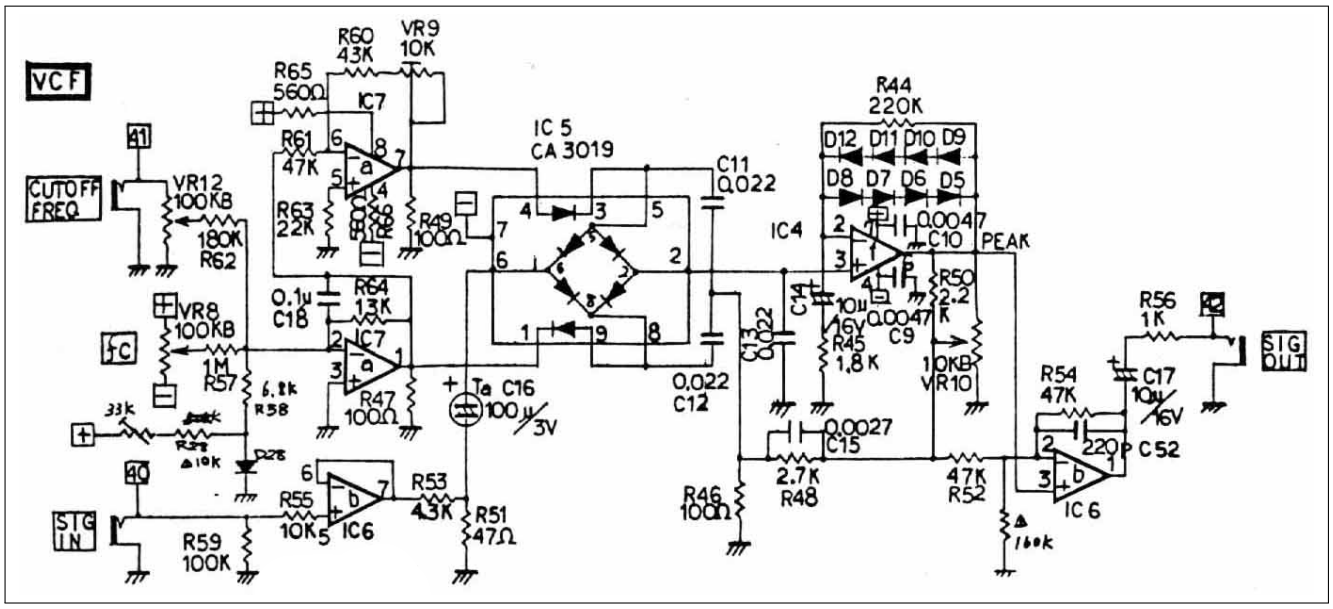

Figure 1: *Original Korg MS-50 VCF circuit adopted from [15].*

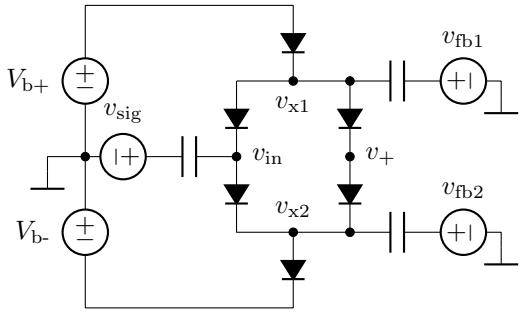

Figure 2: *Voltage controllable diode bridge.*

The basic idea of this topology is based around the small signal behavior of a single diode around its operating point and the resulting dynamic resistance r_d.

To derive an estimate of r_d for a single diode D, let us assume that the total voltage v_D across this diode can be written as a superposition of a constant biasing voltage V_b and a time varying small signal voltage v_s as

$$v_\mathrm{D} = V_\mathrm{b} + v_\mathrm{s} \ , \tag{1}$$

with $v_\mathrm{s} \ll V_\mathrm{b}$. Substituting Eqn. (1) in the ideal diode equation $i_\mathrm{D} = I_\mathrm{S} \cdot e^{\frac{v_\mathrm{D}}{n \cdot v_\mathrm{T}}} - I_\mathrm{S}$ and separating the constant term of the biasing current I_b yields

$$\begin{aligned} i_\mathrm{D} &= I_\mathrm{S} \cdot e^{\frac{V_\mathrm{b}+v_\mathrm{s}}{n \cdot v_\mathrm{T}}} - I_\mathrm{S} \\ &= I_\mathrm{S} \cdot e^{\frac{V_\mathrm{b}}{n \cdot v_\mathrm{T}}} \cdot e^{\frac{v_\mathrm{s}}{n \cdot v_\mathrm{T}}} - I_\mathrm{S} \\ &= I_\mathrm{b} \cdot e^{\frac{v_\mathrm{s}}{n \cdot v_\mathrm{T}}} - I_\mathrm{S} \ . \end{aligned} \tag{2}$$

Assuming also that $v_\mathrm{s} \ll n \cdot v_\mathrm{T}$ we can approximate Eqn. (2) with a first order Taylor expansion around $v_\mathrm{s} = 0\,\mathrm{V}$:

$$\begin{aligned} i_\mathrm{D} \approx I_\mathrm{b} \cdot (1 + \frac{v_\mathrm{s}}{n \cdot v_\mathrm{T}}) - I_\mathrm{S} &= I_\mathrm{b} + \frac{I_\mathrm{b} \cdot v_\mathrm{s}}{n \cdot v_\mathrm{T}} - I_\mathrm{S} \\ &= I_\mathrm{b} + \frac{v_\mathrm{s}}{r_\mathrm{d}} - I_\mathrm{S} \end{aligned} \tag{3}$$

In Eqn. (3), $r_\mathrm{d} = \frac{n \cdot v_\mathrm{T}}{I_\mathrm{b}}$ is now defined as the dynamic resistance at the operating point set by V_b and thus the slope of the tangent at the operating point.

To apply these theoretical conclusions in practice, one must find a way to decouple the biasing voltage and the signal itself for superposition on the diode, as they almost always come from independent sources. One way to accomplish this is capacitive coupling. This is the method taken in the MS-50 filter. Figure 2 shows a simplified diode bridge as in the actual circuit but with ideal voltage sources for all connected voltages and the assumption that the capacitors are sufficiently large to have neglectable AC-impedance for the time-varying input and feedback signals.

Under these assumptions, the diode bridge network can be transformed into a linearized network of equivalent resistors $r_{\mathrm{d}1}$-$r_{\mathrm{d}6}$ and further simplified into fewer resistors by calculating Thévenin equivalence resistances [24].

Figure 3a shows the linearized diode bridge with the bias sources $V_{\mathrm{b}+}$ and $V_{\mathrm{b}-}$ replaced by shorts. The dashed lines show the three different cases for calculating the equivalent resistances r_A, r_B, r_C and r_D seen by the sources v_sig, $v_{\mathrm{fb}1}$ and $v_{\mathrm{fb}2}$ towards nodes $v_{\mathrm{x}1}$, $v_{\mathrm{x}2}$ and v_+ respectively as depicted in Fig. 3b. The equivalent resistances can be found as

$$r_\mathrm{A} = \big((r_{\mathrm{d}4} || r_{\mathrm{d}6}) + r_{\mathrm{d}3} + r_{\mathrm{d}5} \big) \,||\, r_{\mathrm{d}1} \,||\, r_{\mathrm{d}2} \tag{4}$$

$$r_\mathrm{B} = \big((r_{\mathrm{d}1} || r_{\mathrm{d}2}) + r_{\mathrm{d}3} + r_{\mathrm{d}5} \big) \,||\, r_{\mathrm{d}4} \,||\, r_{\mathrm{d}6} \tag{5}$$

$$r_\mathrm{C} = \Big(\big((r_{\mathrm{d}2} + r_{\mathrm{d}4}) \,||\, r_{\mathrm{d}6} \big) + r_{\mathrm{d}5} \Big) \,||\, r_{\mathrm{d}3} \tag{6}$$

$$r_\mathrm{D} = \Big(\big((r_{\mathrm{d}2} + r_{\mathrm{d}4}) \,||\, r_{\mathrm{d}1} \big) + r_{\mathrm{d}3} \Big) \,||\, r_{\mathrm{d}5} \tag{7}$$

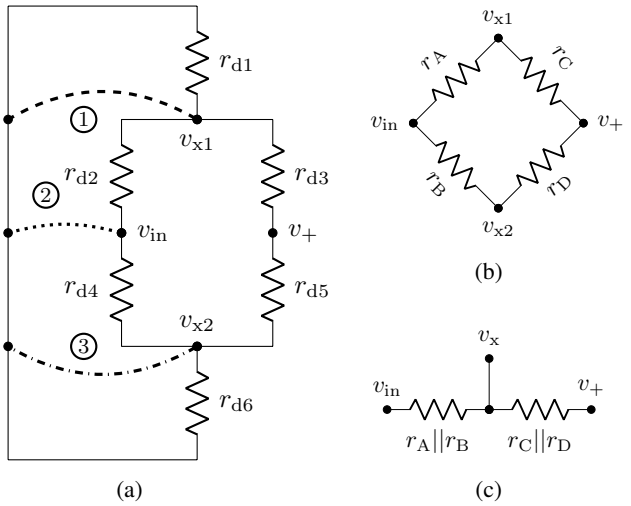

Figure 3: *a) Linearized diode bridge to calculate Thévenin equivalence resistances for all three sources. ① V_{fb1} replaced by a short to ground, ② V_{sig} replaced by a short to ground, ③ V_{fb2} replaced by a short to ground; b) Thévenin equivalent resistances of linearized diode bridge; and c) simplified Thévenin equivalent resistors using symmetry.*

If we further assume that the bridge is symmetrically biased and that the voltage sources v_{fb1} and v_{fb2} are equal as they are fed from the same branch in the original circuit ($v_{x1} = v_{x2}$), the pairs of r_{A} & r_{B} and r_{C} & r_{D} can be further summarized into two resistors with their respective parallel values (see Fig. 3c). Under the aforementioned assumptions we have thus transformed the diode bridge for small signals into two equivalent resistors and have further reduced the symmetric feedback branches into one common node. We will use these results in the next section to point out the Sallen-Key structure of the filter.

2.2. Sallen-Key Topology

Like the MS-20 filter from the same series of synths [19], the MS-50 VCF is also built around a Sallen-Key topology [16]. The Sallen-Key topology has only recently been the subject of study from a virtual analog perspective [25, 26, 27]. Figure 4 shows the relevant parts of the complete schematic with the linearized small signal diode bridge equivalent resistances substituted in. As the diode bridge is driven in the original circuit by two branches via C_{11} and C_{12}, they form a parallel capacitance in the linearized version.

From this circuit, the Sallen-Key topology with two resistive impedances in the forward path and two capacitive impedances on the op-amp input and feedback path is clearly visible, which is the characteristic configuration for a low-pass filter [16]. The variable resistor VR_{10} is additionally added to the standard configuration to control the amount of feedback. In the original schematic an additionally gain factor formed by R_{44} and R_{45} as well as clipping diodes around IC_4 are incorporated, which is omitted in Figure 4 for clarity.

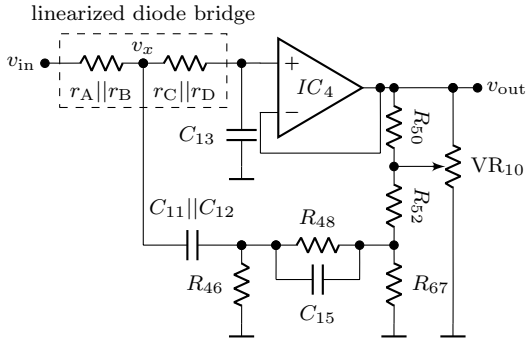

Figure 4: *The filter's simplified, linearized Sallen-Key Structure.*

3. WDF MODEL

Thanks to recent advances in the field of Wave Digital Filters [2, 3, 4, 6] it is possible to make a virtual analog model of such a diode bridge controlled filter including the non-linearities in the feedback path. Figure 5 shows the circuit which is used for modeling, the component values are given in Tab. 1.

Some parts of the original MS-50 schematic were simplified for this model, which are in the signal input, biasing and output stages. In the original circuit, the input signal is terminated by a simple load resistance of $R_{59} = 100\,\text{k}\Omega$ followed by a unity gain amplifier. This stage is modelled as an ideal voltage source in the WDF. The second part which underwent simplifications is the biasing stage. In the original circuit, it consists of two op-amps in a summing configuration with weighted gains. These elements add external, manual and temperature compensation signals to a biasing voltage and its inverse. These voltages are symmetrically fed into the diode bridge. In the WDF model, the biasing op-amps are modelled as voltage sources with an output resistance of $R_{s+} = R_{s-} = 50\,\Omega$ and the biasing signal is treated as one composition of the individual original voltages. The next modification is performed around the main Sallen-Key op-amp IC_4, which originally featured a couple of clipping diodes around its gain feedback path. These ones are omitted from this model to be able to independently study the behavior of the diode ring in the feedback path and its non-linear behavior. Finally, the output voltage is taken across an additional output load resistor R_{L}.

The WDF is created from this circuit using the MNA-based techniques described in [2, 3, 4, 6], especially for the complicated topology, the multiple non-linearities and the ideal op-amps. Figure 7 shows the resulting adaptor structure. All linear components are connected in branches to an $\mathcal{R}$-type adapter at the root. The non-linearities are arranged on the upper side of the adapter and the diodes are modelled using the Shockley model [28]. As there is no detailed datasheet for the CA 3019 diode array, parameter values of $I_s = 2.52\text{e}{-9}\,\text{A}$ and $n = 1.752$ are used based on a 1N4148 fast small signal switching diode. The matrix of the $\mathcal{R}$-type describing the scattering behavior between all ports also incorporates the op-amps as Nullors, which results in ideal op-amp models [6]. The final adapter structure is fully compatible with the current state of the RT-WDF Wave Digital Filter simulation library [17].

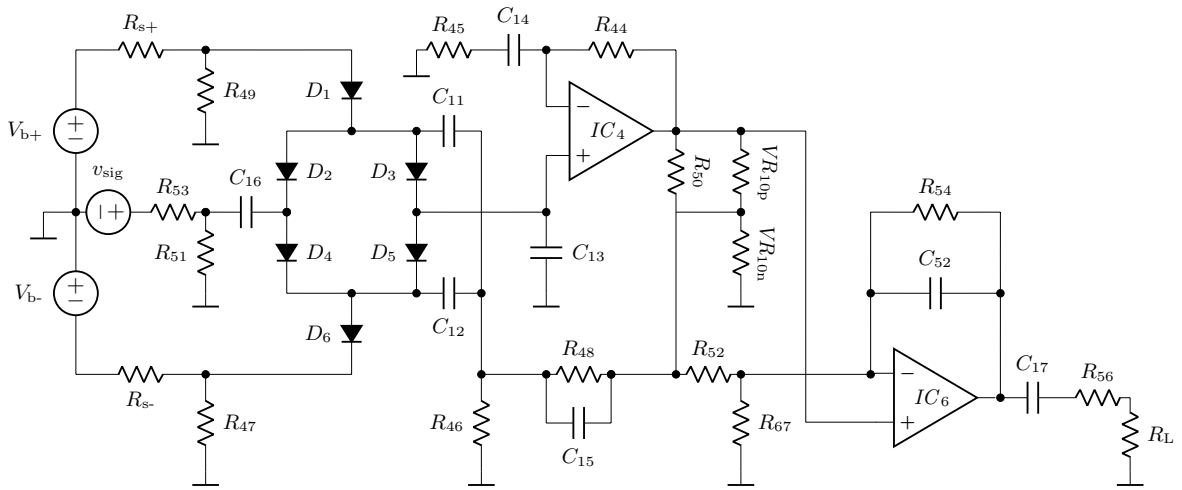

Figure 5: *Simplified VCF circuit used for simulation.*

Table 1: *Component values used for simulation.*

R_{s+}	50 Ω	R_{53}	4.3 kΩ	C_{16}	100 µF
R_{s-}	50 Ω	R_{54}	47 kΩ	C_{17}	10 µF
R_{44}	220 kΩ	R_{56}	1 kΩ	C_{52}	220 pF
R_{45}	1.8 kΩ	R_{67}	160 kΩ	D_1	1N4148
R_{46}	100 Ω	R_L	100 kΩ	D_2	1N4148
R_{47}	100 Ω	VR_{10p}+VR_{10n}	10 kΩ	D_3	1N4148
R_{48}	2.7 kΩ	C_{11}	22 nF	D_4	1N4148
R_{49}	100 Ω	C_{12}	22 nF	D_5	1N4148
R_{50}	2.2 kΩ	C_{13}	22 nF	D_6	1N4148
R_{51}	47 Ω	C_{14}	10 µF	IC_4	ideal
R_{52}	47 kΩ	C_{15}	2.7 nF	IC_6	ideal

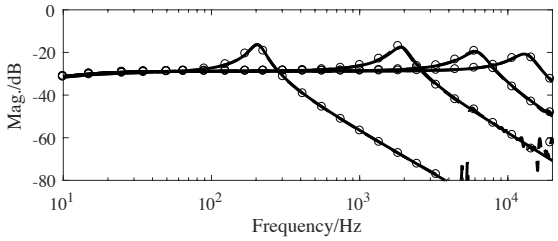

Figure 6: *Mag. spectrum of calculated small-signal (*$50\,\mathrm{mV}$*) impulse responses of the circuit, at several cutoff frequencies. SPICE results are shown with a dotted line. Resonance is fixed at 0.7, bias voltage is set to* $[0.2, 0.3, 0.35, 0.38]\,\mathrm{V}$ *from left to right.*

4. RESULTS

The performance of the model is verified in three ways. Firstly, its linear behavior is measured by taking a small-signal impulse of $50\,\mathrm{mV}$ and processing it with both the WDF model and an equivalent SPICE model of the circuit from Fig. 5 in LTspice. This impulse produces a voltage on the right end of C_{16} of around $0.5\,\mathrm{mV} \ll n \cdot v_\mathrm{T}$, which keeps the diodes in an approximately linear region (see Sec. 2.1). The produced response thus characterizes the filter behavior in the linear region. Fig. 6 shows the magnitude responses of several such impulses for constant resonance setting and sweeping cutoff frequency. The match between the described WDF model and SPICE is good, with the exception of the presence of some small anomalies in the SPICE model, caused by the resampling algorithm used. The sampling rate of the WDF simulation was 176.4 kHz.

Secondly, the nonlinear behavior of the model is tested by examining its resonant behavior when driven by signals of varying amplitude. A sawtooth signal of 50 Hz is chosen for this purpose. Fig. 8 shows the output of the model and the equivalent SPICE model. Clearly visible with increasing input amplitude is the exaggeration of the initial transient of the sawtooth waveform while the following resonant behavior stays relatively constant. The output signals of the presented WDF model and SPICE are very close.

In order to further examine the variation in resonance frequency and amplitude with input level, a further test was performed. The filter was given a resonance setting of 0.85, which produces self-oscillation. The filter input was then driven with a ramp waveform, peaking at 2 V, and the changing character of the self-oscillation observed. Fig. 9 shows the results of this process. The instantaneous frequency and amplitude of the output are estimated using a Hilbert transform of the output signal. The estimates are smoothed to remove higher frequency components that relate to the waveshape of the self-oscillation rather than the fundamental. The instantaneous frequency of the output is seen to decrease as the input ramp increases in voltage and thus re-biases the diode bridge, starting at around approximately 250 Hz and falling to approximately 200 Hz. The instantaneous amplitude of the output drops as the input voltage increases, with the self-oscillation almost completely damped as the input gets close to 2 V. Agreement between the SPICE and WDF models is close by these measures.

4.1. Performance

The maximum count of iterations for the six-dimensional nonlinear system in the Newton Solver with a stopping criteria of $\|\mathbf{F}\| \leq 1.5\mathrm{e}{-9}$ did not exceed 2 at any time during calculation of the results presented here. No damping steps were needed. An increase of iterations was mostly noticed on sharp transients in the input signal and zero crossings of the output signal, both of which cause switching between the diodes.

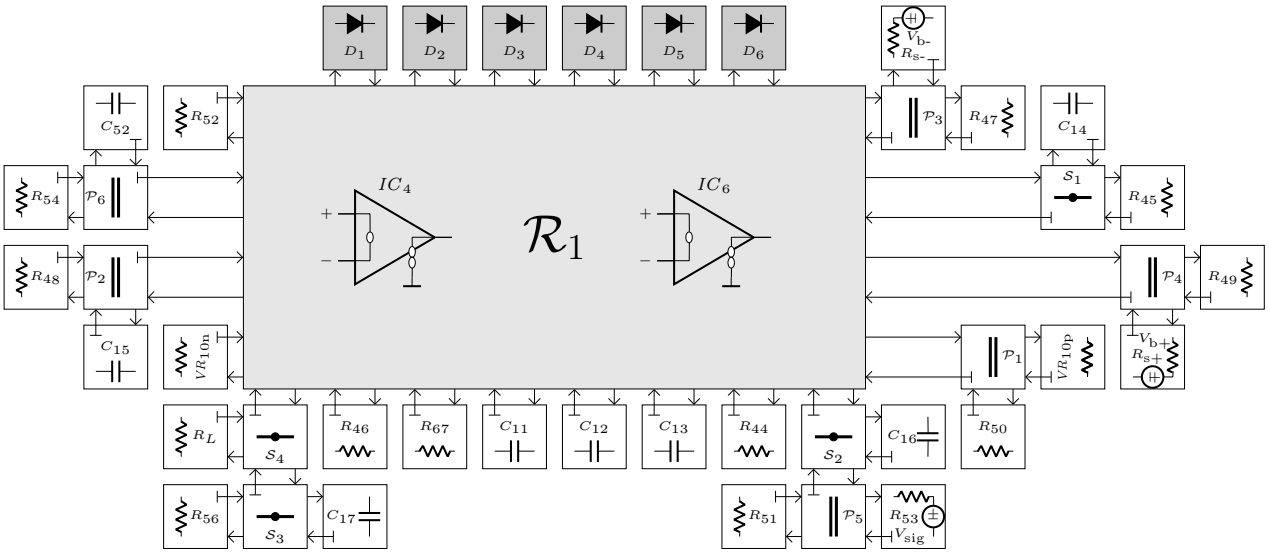

Figure 7: *WDF Adaptor Structure.*

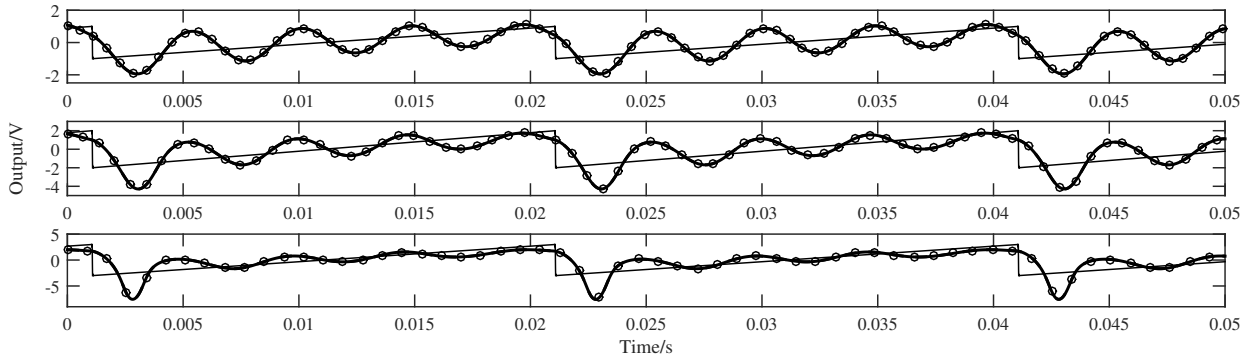

Figure 8: *Output of model when driven by a* 50 Hz *sawtooth waveform of peak-to-peak amplitude of top:* 1 V *middle:* 2 V*, bottom:* 3 V*. SPICE results are shown with dots. Resonance is set to 0.8, and the bias voltage is* 0.2 V*. The input sawtooth is shown as a reference.*

In terms of computational load, the implementation in RT-WDF [17] consumes approx. 80 % of one core at a sampling rate of 176.4 kHz on a laptop computer from 2013 with Intel i7 2.4 GHz CPU (4 cores) and 8 GB RAM running OS X 10.11.4. The *wdfRenderer* [17] was built with Apple LLVM 7.1 at optimization level `-O3` and ran with a single rendering thread without any other considerable applications in the background or performance tweaking.

5. CONCLUSION

The circuit of the *Korg* MS-50 voltage controlled filter was examined, and shown to fundamentally be a form of the Sallen-Key topology, controlled by a highly non-linear diode bridge. A Wave Digital Filter model of a simplified circuit was presented to highlight the influence of the diode bridge on the filter behavior and shown to match in most parts a reference implementation in SPICE. For small signal linear frequency analysis, small differences are mostly seen in terms of frequency warping effects in the WDF and aliasing artifacts in the SPICE results. Nonlinear frequency and amplitude variations exhibited by the filter are examined, with close agreement between the SPICE reference model and the WDF model shown. The model was implemented using the RT-WDF C++ framework, and is able to be run in real-time. Future research should analyze the original filter circuit behavior including the amplitude limiting clipping diodes and take advantage of the simplified diode bridge structure from Sec. 2 for a simplified model.

6. ACKNOWLEDGMENTS

Many thanks to Ross W. Dunkel for delightful initial discussions! Also, thanks to all reviewers for detailed comments.

7. REFERENCES

[1] A. Fettweis, "Wave digital filters: Theory and practice," *Proc. IEEE*, vol. 74, no. 2, Feb. 1986.

[2] K. J. Werner, J. O. Smith III, and J. S. Abel, "Wave digital filter adaptors for arbitrary topologies and multiport linear

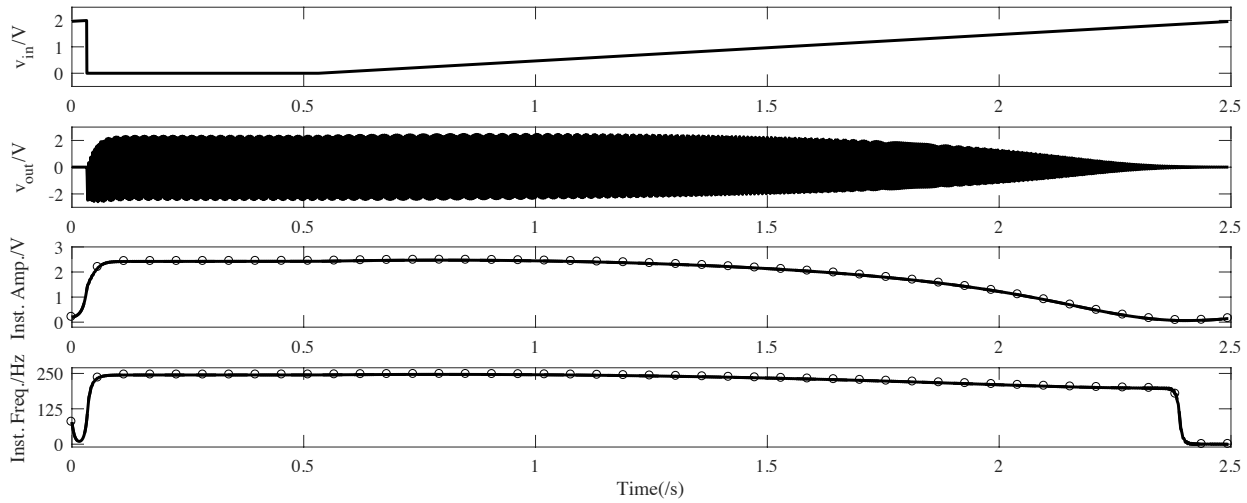

Figure 9: *Output of models when set to self-oscillate with resonance of 0.85 and bias voltage of* $0.2\,\mathrm{V}$*, driven by a slow* $2\,\mathrm{V}$ *ramp input. The input ramp* v_{in}*, model output* v_{out}*, and the estimated instantaneous frequency and amplitude of* v_{out} *are shown. SPICE results are shown with dots.*

elements," in *Proc. Int. Conf. Digital Audio Effects (DAFx-15)*, Trondheim, NOR, Nov. 30 – Dec. 3 2015.

[3] K. J. Werner, V. Nangia, J. O. Smith III, and J. S. Abel, "Resolving wave digital filters with multiple/multiport nonlinearities," in *Proc. Int. Conf. Digital Audio Effects (DAFx-15)*, Trondheim, NOR, Nov. 30 – Dec. 3 2015.

[4] M. J. Olsen, K. J. Werner, and J. O. Smith III, "Resolving grouped nonlinearities in wave digital filters using iterative techniques," in *Proc. Int. Conf. Digital Audio Effects (DAFx-16)*, Brno, CZ, Sept. 5–9 2016.

[5] A. Bernardini, K. J. Werner, A. Sarti, and J. O. Smith, "Modeling a class of multi-port nonlinearities in wave digital structures," in *Proc. 23th Europ. Signal Process. Conf. (EUSIPCO)*, Nice, FR, Aug. 31 – Sept. 4 2015.

[6] K. J. Werner, W. R. Dunkel, M. Rest, M. J. Olsen, and J. O. Smith III, "Wave digital filter modeling of circuits with operational amplifiers," in *Proc. 24th Europ. Signal Process. Conf. (EUSIPCO)*, Budapest, HU, Aug. 29 – Sept. 2 2016.

[7] R. C. D. Paiva, S. D'Angelo, J. Pakarinen, and V. Valimaki, "Emulation of operational amplifiers and diodes in audio distortion circuits," *IEEE Trans. Circuits Syst. II: Exp. Briefs*, vol. 59, no. 10, Oct. 2012.

[8] K. J. Werner, V. Nangia, A. Bernardini, J. O. Smith, III, and A. Sarti, "An improved and generalized diode clipper model for wave digital filters," in *Proc. 139th Conv. Audio Eng. Soc (AES)*, New York, NY, USA, Oct. 29 – Nov. 1 2015.

[9] A. Bernardini and A. Sarti, "Biparametric wave digital filters," *IEEE Trans. Circuits Syst. I: Reg. Papers*, 2017, To be published, DOI: 10.1109/TCSI.2017.2679007.

[10] M. Rest, W. R. Dunkel, K. J. Werner, and J. O. Smith, "RT-WDF—a modular wave digital filter library with support for arbitrary topologies and multiple nonlinearities," in *Proc. Int. Conf. Digital Audio Effects (DAFx-16)*, Brno, CZ, Sept. 5–9 2016.

[11] W. R. Dunkel, M. Rest, K. J. Werner, M. J. Olsen, and J. O. Smith III, "The Fender Bassman 5F6-A family of preamplifier circuits—a wave digital filter case study," in *Proc. Int. Conf. Digital Audio Effects (DAFx-16)*, Brno, CZ, Sept. 5–9 2016.

[12] K. J. Werner, *Virtual Analog Modeling of Audio Circuitry Using Wave Digital Filters*, Ph.D. dissertation, Stanford University, Stanford, CA, USA, Dec. 2016.

[13] J. Parker, "A simple digital model of the diode-based ring-modulator," in *Proc. Int. Conf. Digital Audio Effects (DAFx-11)*, Paris, FR, Sept. 19–23 2011.

[14] A. Bernardini, K. J. Werner, A. Sarti, and J. O. Smith III, "Modeling nonlinear wave digital elements using the Lambert function," *IEEE Trans. Circuits Syst. II: Reg. Papers*, vol. 63, no. 8, Aug. 2016.

[15] KORG, *Model MS-50 Circuit Diagram*, Nov. 1978.

[16] R. P. Sallen and E. L. Key, "A practical method of designing RC active filters," *IRE Trans. Circuit Theory*, vol. 2, no. 1, Mar. 1955.

[17] M. Rest, W. R. Dunkel, and K. J. Werner, "RT-WDF—a modular wave digital filter library," 2016–2017, Available at https://github.com/RT-WDF, accessed Mar. 12 2017.

[18] A. Vladimirescu, *The SPICE Book*, John Wiley & Sons, New York, NY, USA, 1994.

[19] T. Stinchcombe, "A study of the Korg MS10 & MS20 filters," Online, Aug. 30 2006, http://www.timstinchcombe.co.uk/synth/MS20_study.pdf, accessed Mar. 12 2017.

[20] Y. Nagahama, "Voltage-controlled filter," Aug. 2 1977, US Patent 4,039,980.

[21] AMSynths on ModularGrid, "AM8319," Online, Oct 30 2012, https://www.modulargrid.net/e/amsynths-am8319, accessed June 20 2017.

[22] RCA, *CA-3119 Ultra-Fast Low-Capacitance Matched Diodes*, Datasheet. RCA Corporation, Mar. 1970.

[23] B. Brannon, *ICAN-5299 Application of the RCA-CA3019 Integrated-Circuit Diode Array*, RCA Linear Integrated Circuits and MOSFETS Applications. RCA Corporation, 1983.

[24] A. S. Sedra and K. C. Smith, *Microelectronic Circuits*, Oxford University Press, New York, NY, USA, 5th edition, 2004.

[25] J. Parker and S. D'Angelo, "A digital model of the Buchla lowpass-gate," in *Proc. Int. Conf. Digital Audio Effects (DAFx-13)*, Maynooth, IE, Sept. 2–5 2013.

[26] K. J. Werner, J. S. Abel, and J. O. Smith III, "The TR-808 cymbal: a physically-informed, circuit-bendable, digital model," in *Proc. Int. Comput. Music Conf. (ICMC)*, Athens, EL, Sept. 14–20 2014.

[27] M. Verasani, A. Bernardini, and A. Sarti, "Modeling Sallen-Key audio filters in the wave digital domain," in *Proc. IEEE Int. Conf. Acoust., Speech, Signal Process. (ICASSP)*, New Orleans, LA, USA, Mar. 5–9 2017.

[28] S. M. Sze, *Physics of semiconductor devices*, John Wiley & Sons, New York, NY, USA, 2nd edition, 1981.